Identification of elastic-plastic behavior in AHSS using the isotropic hardening model by the finite element method and EBSD

Érika Aparecida da Silva[a], Marcelo dos Santos Pereira[a], Jean Pierre Faye[b], Rosinei Batista Ribeiro[c,d], Nilo Antonio de Sousa Sampaio[e], José Wilson de Jesus Silva[d]

[a]Universidade Estadual Paulista – UNESP - Campus de Guaratinguetá,Guaratinguetá, SP, Brazil.
[b]Ecole Nationale d'Ingénieurs de Tarbes, ENIT, Institut National Polytechnique de Toulouse, INPT, France.
[c]Instituto Tecnológico de Aeronáutica – ITA – São José dos Campos, SP, Brazil
[d]Centro Universitário Teresa D'Ávila – UNIFATEA – Lorena, SP, Brazil
[e]Universidade do Estado do Rio de Janeiro – UERJ – Resende, RJ, Brazil

Abstract— The aim of this work is to analyze the maximum potential for use of isotropic hardening model in the determination of elastoplastic behavior in an advanced high strength steel (AHSS) known as dual phase steel, with yield stress of 780 MPa. This material belongs to a class of steels currently used the feedstock in the production of vehicles. This material was chosen because it has a high elastic return or spring back effect, which commits the mass production of components, causing dimensional failures in projects. Consequently, it is a steel that presents a complex microstructural behavior during deformation. Mechanical properties of the material were evaluated by tensile tests. Mechanical characterization of spring back effect was carried out by means of sheet metal forming, called three-point air bending. These results were compared with results obtained by the Finite Element Analysis, using the isotropic hardening model. Microstructures were analyzed by means of EBSD technique and the structural fractions resulting from mechanical bending processes were identified, as well as, one of the main mechanisms of reorganization of the crystalline reticulum, measured by CSL boundaries, was identified. The 2D simulation and the isotropic hardening model used in ABAQUS was efficient to identify the mechanical response of steel in relation to its plastic deformation, concluding that it has a kinematic type hardening. However, such a model used in ABAQUS was not totally satisfactory to predict the degree of spring back, since such a model does not take into account reduction in the Young's modulus present in the AHSS.
Keywords— Spring back; AHSS; Sheet metal forming; finite element analysis; high strength steels, EBSD.

Resumo—El objetivo de este trabajo es analizar el potencial máximo para el uso del modelo de endurecimiento isotrópico en la determinación del comportamiento elastoplástico en un acero avanzado de alta resistencia (AHSS) conocido como acero de fase dual, con un rendimiento de 780 MPa. Este material pertenece a una clase de aceros utilizados actualmente como materia prima en la producción de vehículos. Se eligió este material porque tiene un alto efecto de retorno elástico o recuperación elástica, lo que compromete la producción en masa de componentes, lo que provoca fallas dimensionales en los proyectos. En consecuencia, es un acero que presenta un complejo comportamiento microestructural durante la deformación. Las propiedades mecánicas del material fueron evaluadas mediante ensayos de tracción. La caracterización mecánica del efecto springback se llevó a cabo mediante la conformación de chapa metálica, denominada flexión por aire de tres puntos. Estos resultados se compararon con los resultados obtenidos mediante el análisis de elementos finitos, utilizando el modelo de endurecimiento isotrópico. Las microestructuras se analizaron mediante la técnica de EBSD y se identificaron las fracciones estructurales resultantes de los procesos de flexión mecánica, y se identificó uno de los principales mecanismos de reorganización del retículo cristalino, medido por los límites de CSL. La simulación 2D y el modelo de endurecimiento isotrópico utilizado en ABAQUS fueron eficientes para identificar la respuesta mecánica del acero en relación con su deformación plástica, concluyendo que tiene un endurecimiento de tipo cinemático. Sin embargo, tal modelo utilizado en ABAQUS no fue totalmente satisfactorio para predecir el grado de recuperación, ya que dicho modelo no tiene en cuenta la reducción en el módulo de Young presente en el AHSS.
Palabras clave: Springback; AHSS; Conformado de chapa metálica; análisis de elementos finitos; Aceros de alta resistencia, EBSD.

I. INTRODUCTION

Due to the need for production of new materials for automotive industry with better performance coupled with concern for environmental issues, aiming at reducing the consumption of fossil fuels, emerged, from the 1990s, advanced high strength steels (AHSS), which reconcile a small sheet thickness and high mechanical strength [1].

Current issues in the automotive industry are closely related to environmental and energy issues, such as the emission of greenhouse gases (GHG emissions). Research shows a trend toward a reduction in GHG emissions by 2025 from the use of vehicles made with AHSS and new designs for fuel economy [2].

However, the mass production of structural components is limited due to the challenges in the formability and union of plates due to elastic return known as springback effect[3].

The springback can be identified as a change in shape of part subjected to unloading and after the withdrawal of the forming tool due to a redistribution of residual elastic stresses. This phenomenon is characteristic of the new steels with high resistance in relation to traditional steels of low resistance. Thus, the automobile industry has sought to use differentiated materials and modify manufacturing processes in an attempt to minimize problems with the springback effect [4].

Now, computational simulation by Finite Element Analysis (FEA) is one of the most used tools in projects for the evaluation of conformation processes. The main difficulty in the use of FEA is regarding AHSS due to the occurrence of several nonlinear phenomena during plastic deformation. The main factor that causes this nonlinearity in the behavior of these steels is the phenomenon of modulus of elasticity during discharging [3].

Several works [5-7] used the conventional isotropic hardening model to determine the degree of springback and resulted in an overestimation of those values, also realized that such results can be improved with inclusion of the Bauschinger effect, which affects the variation of Young's modulus.

Thus, the present work has chosen to use the 2D simulation, which presents a finite element superior mesh than 3D simulation. The model used for simulation was the isotropic hardening. The objective was to identify the behavior of elastoplasticity present in the DP780 steel with the aid of the study of microstructural parameters obtained by means of backscattered electron technique (EBSD). It is known that a greater knowledge about plasticity behavior of a material allows the development of new simulation models that improve the prediction of springback effect.

II. EXPERIMENTAL PROCEDURE

2.1. Tensile tests

Values for mechanical properties have been obtained by means of tensile tests, extracting specimens in the rolling direction of material, using the standard ASTM E8M-11. Tests have been carried out in a universal test machine, Instron.

2.2. Sheet metal forming

Test specimens were made from the same material as received and sectioned at dimensions following: 80 mm long by 30 mm wide. Such dimensions of specimens were made according to parameters defined for the unconstrained cylindrical bending test presented at the Numi sheet conference 2002 [8].The three-point air bending was carried out in accordance with the norms ASTM E290-09. The values selected for the internal angle bending were: 30 and 90 degrees, respectively, for each bend. The punch was removed from the material 20 seconds after reaching the bending angle and then the measurement was made of the new bend angle to determine whether there was springback. For this measurement, it was used the software ImageJ 1.45 for processing images photographed on LaserLevel 2.0.1 application, according to Figure 1. Such measurements continued to be made for a period of 12 h, 24 h, 48 h, 72 h and 96 h after forming. Completed the 96 h after mechanical bending, the angle bending resulting was subtracted from the initial angle of bending, which were 30º or 90º, and this subtraction resulted in total springback angle.
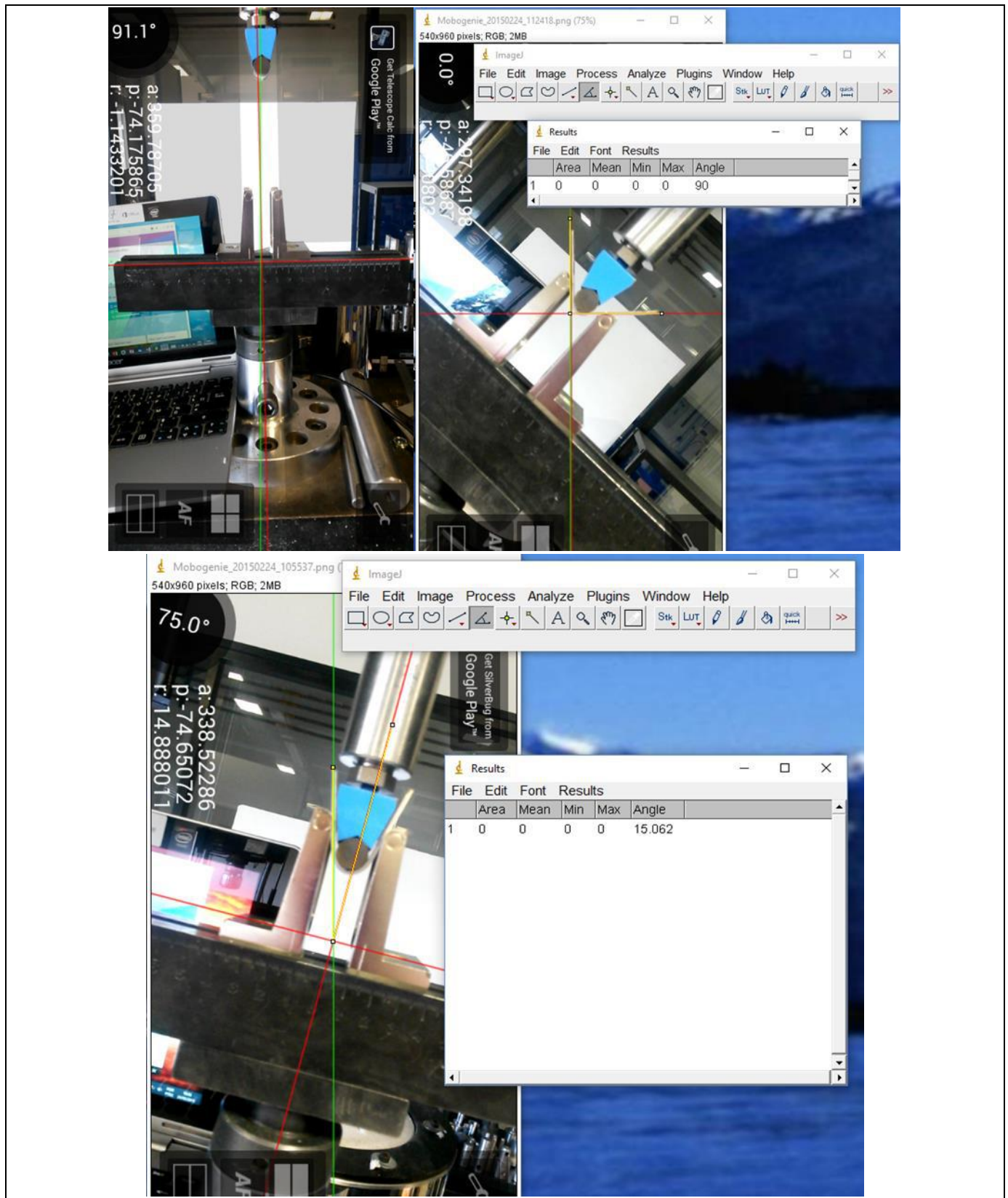
Softwares: LaserLevel and ImageJ

Fig.1. (a) Android camera leveling in relation to the Instron bending device(b) and (c) Comparison between the angular value provided by LaserLevel and ImageJ for sheet metal forming at 90° and 30°, respectively.

2.3. Finite element analysis - FEA

Simulation of sheet metal forming and later springback effect was carried out using the software ABAQUS finite elements/CAE 6.13-2. The model used in all simulations carried out in this work was the model of isotropic hardening, taking into consideration the Young´s modulus of materials, its Poisson's coefficient, mass density, true stress and true strain. It was assumed a solid and homogeneous steel for composition of the die and the punction with a ratio of 0.03 between tension plan and deformation in the thickness. It was used a mesh size of 0.0002, with a control of curvature (H/L) in the value of 0.1, which is the same value as the fraction of total size used and with the analysis of 8 elements per cycle.
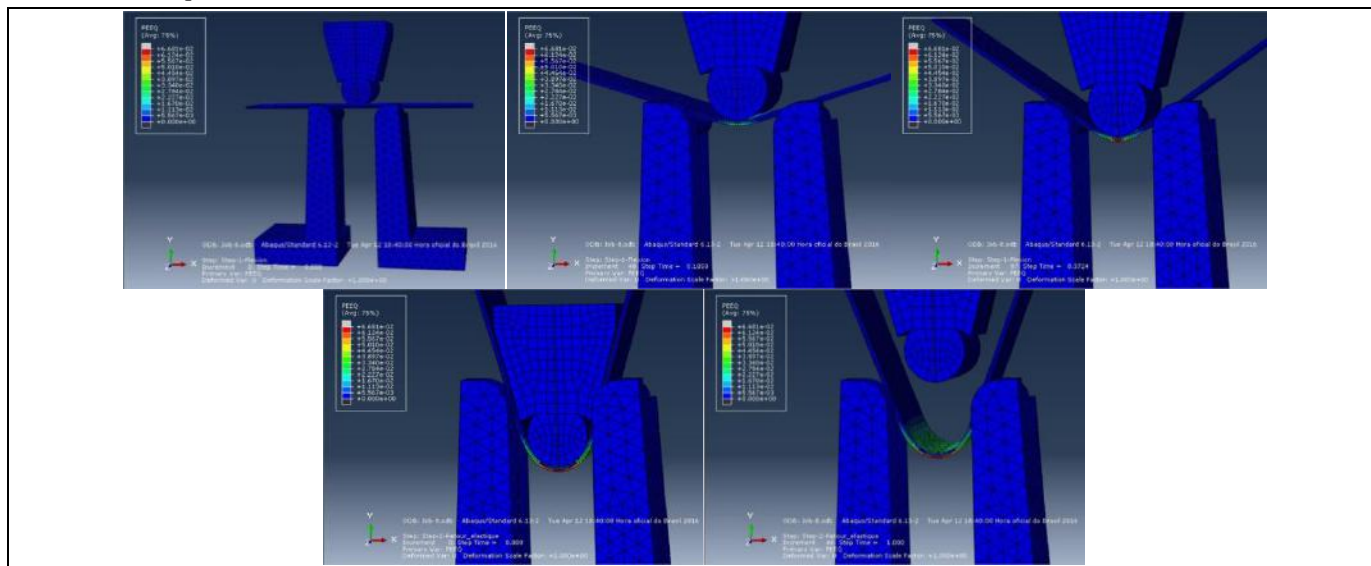
Software: Abaqus CAE 6.14

Fig.2. Stages of sheet metal forming in ascending order from left to right. Simulation carried out in the ABAQUS, isotropic model for the DP 780 steel folded at 30°.

2.4. Electron backscatter diffraction - EBSD

EBSD is a technique performed inside scanning electronic microscope when positioning a sample of perfectly flat surface by tilting it to 70 degrees with the incident of the electron beam [9]. It was used a scanning electronic microscope with field emission, model JSM-7000F, JEOL manufacturer, software Channel 5, Oxford Instruments HKL, equipped for analyzes of EBSD. In this step, the samples were analyzed in the dimensions of 15 mm length x 5 mm width on the two surfaces: external and along the thickness, following the rolling direction of sheets.

III.   RESULTS AND DISCUSSION

Mechanical properties

Regarding mechanical properties, their values, shown in Table 1, were obtained by tensile tests. In Table 1, tensile strength is designed by RT in MPa, yield strength by LE in MPa, elongation by Elong in ε%, Young's modulus by E in GPa and modulus of resilience by Ur in KPa.

Table.1: Mechanical properties of DP780 steel.

Steel	RT (MPa)	LE (MPa)	ε%	E (GPa)	Ur (KPa)
DP780	864.43 ± 31	604.90 ± 1,9	23.73 ± 3.3	204.45 ± 1.02	894.83 ± 1.02

Sheet metal forming and FEA

Table 2 presents the final values of internal bending angles after finalization of the sheet metal forming, measured from 0 seconds to 96 hours after relief of tensions. Note that as expected according to the literature and in agreement with previous studies of the same research group, the values of these angles increase according to degree of resistance and resilience of materials.

Table.2: Internal bending angles from 0 seconds to 96 hours after the strain relief, from the initial angle of 30° and chosen their respective values of standard deviation.

30°						
Steel	**0 s**	**20 s**	**24 h**	**48 h**	**72 h**	**96 h**
DP780	29.88 ± 0.73	47.14 ± 0,34	49.07 ± 0.88	50.34 ± 1.9	50.47 ± 1.84	50.65 ± 1.8
90°						
DP780	88.62 ± 0.99	104.9 ± 0.29	105.02 ± 0.4	105.27 ± 0.45	105.29 ± 0.44	105.32 ± 0.44

Figure 3 below shows a comparison between experimental values of angles of springback obtained by the sheet metal forming and values obtained by FEA.

As expected (blue line), springback values were higher for treatments carried out at 30°, since a sheet metal forming performed in a more acute angle (30°) demands a greater tension amount, resulting in greater quantity of elastic residual tension and consequently greater springback effect. Therefore, the steel when bent at 30° obtained 2.236° more at its springback angle.

However, when observing the results from FEA (red line), it is noted that for the treatment at 90°, the springack value was overestimated at 1.756° and for the treatment at 30°, the springback value was underestimated at 2.127°. Although this difference is not so great, it is necessary to assert that the hardening model used is not ideal for predicting the degree of springback for this type of material.
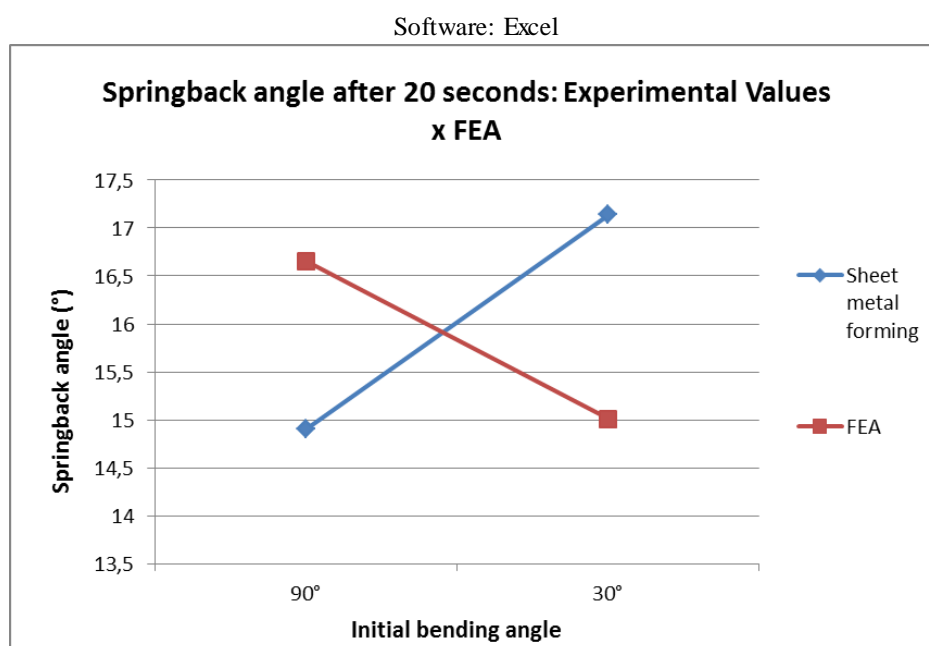
Software: Excel

Fig.3: Comparison between experimental and calculated springback angles for the sheet metal forming in the 30° and 90° for DP780 steel.

In Figure 4, it is displayed results provided by ABAQUS for Von Mises Stress in Pa (S, Mises) and plastic deformation equivalent (PEEQ), after the effect springback, for sample submitted to sheet metal forming with initial internal angle of 30°.
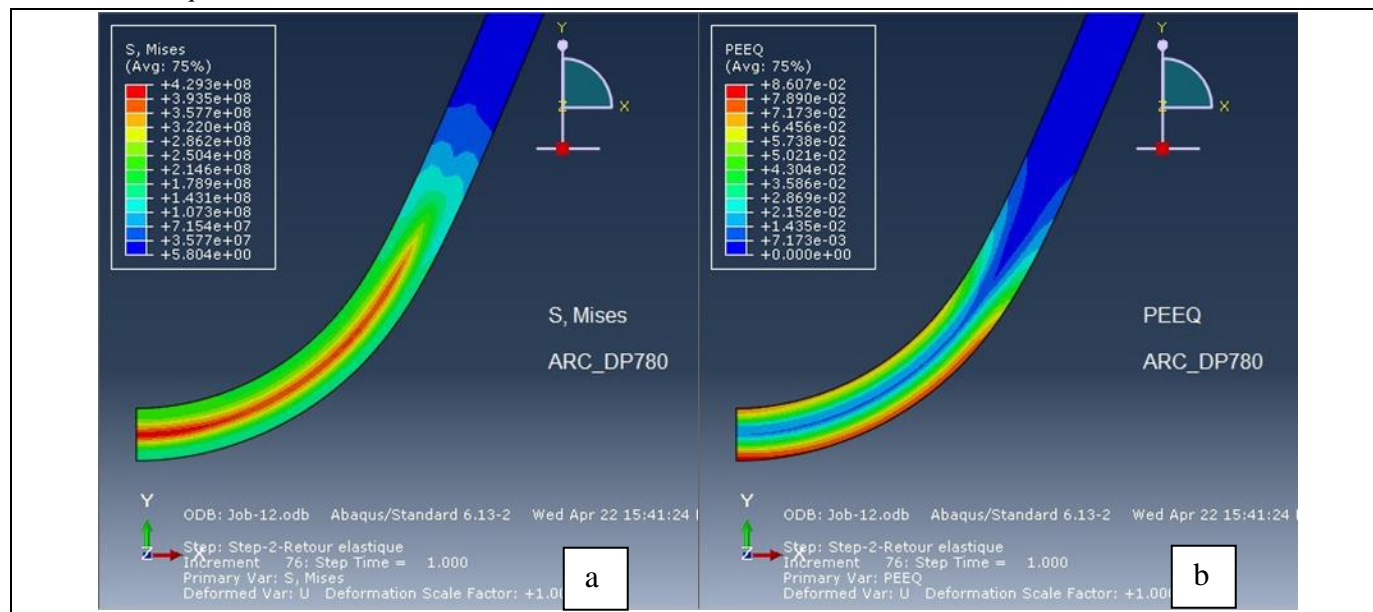
Software: Abaqus CAE 6.14

Fig.4.(a) Von Mises Stress; (b) Equivalent Plastic Deformation Values (PEEQ). DP780 steel after simulation of sheet metal forming at 30° and subsequent springback.

When looking at the region of neutral line, in Figure 4a, there is an orange-reddish solid line in this region, presenting a value of $4.293e^{+8}$ for Von Mises Stress and still in this region, in Figure 4b, it is possible to visualize a light blue color, presenting a value of $7.173e^{-3}$ for equivalent plastic deformation.

With respect to Figure 4b, this steel deformed intensely on surface, but in the region of nucleus (neutral line), it presented a minimal deformation, almost null, throughout the length of the sample. This may help explain the high springback effect, since the material has been shown to be virtually unchanged in the neutral region, due to a higher elastic return of grains during the relief of loads. In addition, it should be also considered that this material has a higher yield stress, and a greater amount of stress is required to cause plastic deformation during the start of sheet metal forming test, resulting in greater elastic residual energy and consequently, greater springback effect.

In addition, DP780 steel has a high resilience value (894,83 KPa) and consequently presents a high springback value, indicating that it absorbed more energy in the elastic deformation and released it after sheet metal forming, without deforming plastically in the region of neutral line. However, when analyzing the region of the outer surface, a higher plastic deformation is verified when compared to region of neutral line, presenting a value around $8.607e^{-2}$.

With respect to Von Mises Stress, it is necessary to know that its value represents the combination of the main tensions in the material pre-existent to the flow,

which starts when this combination reaches the value of the yield stress. Furthermore, it is known that this Von Mises Stress does not distinguish between compressive stress and tensile strength. Since such analysis is done after the elastic return, the Von Mises Stress seen in figure represents the combination of the resulting principal stresses in the material after its deformation and load relief. It is verified that the regions less affected by the plastic deformation, after mechanical folding, resulted in higher value of Von Mises Stress. This indicates that the higher the Von Mises Stress value on the neutral line of the material, the higher the flow should be on this material. Consequently, the release of residual elastic energy within the sample thickness was greater, as well as the plastic deformation on its surface. Thus, it can be said that in this region of neutral line, the higher value of Von Mises Stress represents the greater amount of elastic residual tension in this same region, which is responsible for the springback effect.

According to some authors [10-11], unlike isotropic hardening, the modulus of yield stress during reverse loading is lower than the initial loading. In this case, there is a decrease in flow resistance during reloading caused by this type of hardening. Plasticity for both initial and reverse loading is controlled by different mechanisms, resulting in kinematic type hardening. This confirms observation of the Von Mises Stress in neutral line region immediately after the sheet metal forming, which presented a high value of Mises indicating a greater proximity of yield stresstowards reverse deformation, so that the yield stress is reached quickly by having a smaller

modulus in the direction of unloading when considering the kinematic hardening. Since the hardening of kinematic type reaches a lower modulus of yield stress in the direction of unloading, which facilitates the total release of residual stresses during this step, resulting in the lowest possible value of plastic deformation (PEEQ) in this region of neutral line and consequently the discharge energy is transmitted to the surface resulting in a high plastic deformation (PEEQ) intensity in the regions closest to the surface, whose grains were rearranged by absorbing this energy.

EBSD analysis

A key parameter provided by the EBSD technique is the Coincidence Site Lattice (CSL). CSLs are interfaces in which a given wide angle orientation relationship between adjacent crystals produces a low interfacial energy value. The geometric model of CSLs is based on the formation of a network of sites belonging to the two adjacent networks when interpenetrated, having a relative disorientation between them well determined.

The symbol Σ is used to describe coincidence sites, always followed by odd numbers. The lower this value, the more ordered is the contour. Such a value can be interpreted as the ratio between the volume of the original unit cell of the lattice and the volume of the unit cell of the super-lattice formed by the occurrence of CSL, since the sites of coincidence give rise to a new lattice.

All the following analyzes of the CSLs can be confirmed in Table 3, from verification of degree of disorientation present in these microstructures. Figure 5a Software: Tango (EBSD)

differs from the others because it has a higher intensity of low angle CSLs ($\Sigma 3$ and $\Sigma 7$), showing that the outer surface region presents a higher order of grains crystallographically (misorientation degree of 0.71°). The region along the thickness analyzed before the sheet metal forming in 5b shows an increase in intensity at sites $\Sigma 11$, $\Sigma 25b$, $\Sigma 35a$, $\Sigma 39a$ and $\Sigma 43a$, which are high angle sites, resulting in a greater crystallographic disorder of grains (misorientation degree is higher, 1.02°). It is verified that after folding, in this same region along the thickness, as shown in 5c, the intensity of the high angle sites remains high, but the low angle sites $\Sigma 3$ and $\Sigma 7$ suffer a slight increase, indicating that after the folding, the grains of this region presented a tendency to the greater ordering of their grains (misorientation degree of 0.95°).

Thus, it can be concluded that the mechanical bending process, for this steel, contributed to slightly increase the degree of crystallographic ordering of its grains.

Table.3: Degree of disorientation (misorientation) before and after sheet metal forming at 30° for DP780 steel.

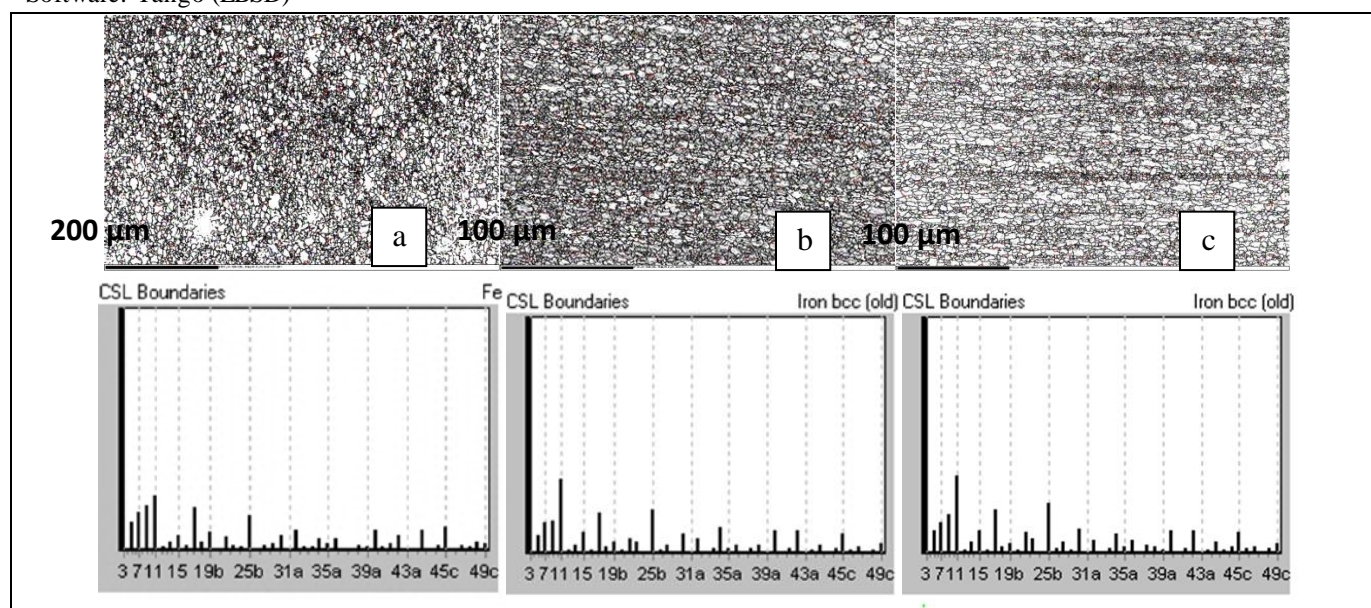| Misorientation degree (°) before and after Sheet Metal Forming		
Steel		DP780
Before sheet metal forming	External surface	0.71 $\pm$ 0.41
	Thickness surface	1.02 $\pm$ 0.68
After sheet metal forming	Thickness surface	0.95 $\pm$ 0.65

Fig.5: Occurrence of Coincident Site Lattices for DP780 steel. (a) region along the outer surface before the sheet metal forming (b) region along the thickness before the sheet metal forming (c) region along the thickness after the sheet metal forming.

When studying the fraction type predominant in each treatment step, it is verified, according to Figure 6, that a lower CSL value results predominantly in fraction of the recrystallized type (6a), a higher CSL value results predominantly in the fraction deformed fraction (6b) and an intermediate CSL value results predominantly in the substructured fraction (6c).

Therefore, it can be concluded that a high degree of crystallographic ordering of the grains is related to structure of the recrystallized type, and a medium and low degree of ordering are related to the substructured and deformed structures.
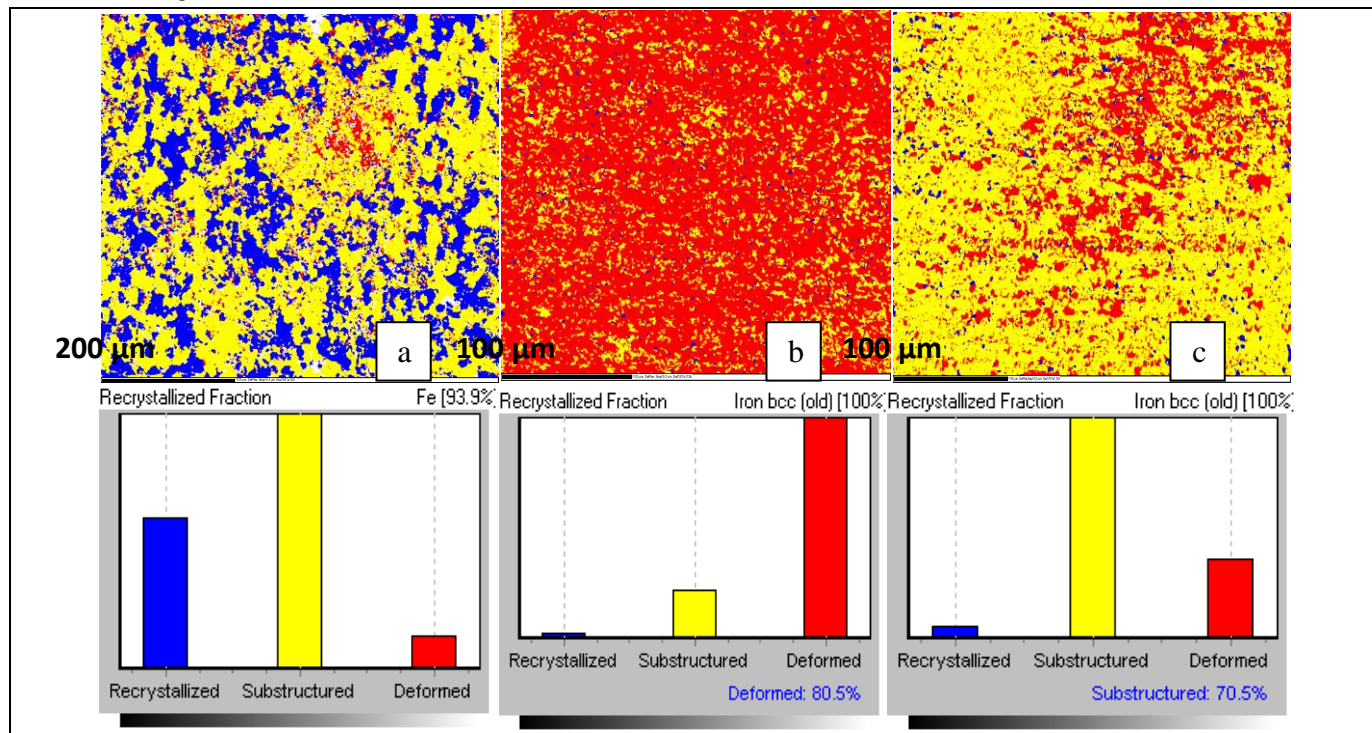
Software: Tango (EBSD)

Fig.6: Types of structural fractions. (a) and (b) external surface and region along the thickness respectively before sheet metal forming. (c) region along the thickness after sheet metal forming at 30°.

Note that previously recrystallized or deformed grains present a large number of dislocations formed mainly as a result of the rolling process, and there is a tendency of these dislocations present in the area of grain contours to reorganize and give rise to a new subset of grains called substructured fraction. The driving force that makes this transformation possible is the elastic residual energy stored during the mechanical conformation process, which is trapped within the grains and through the energy gradient between the interstitial defects within the grains and the edge dislocations, this energy is released during the mechanical unloading, allowing the

grains near the surface of the sample to reorganize into new contours, thus forming the substructured fraction.
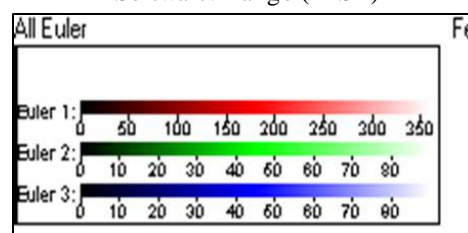
Software: Tango (EBSD)

Fig.7: RGB color legend according to the intensity of the Euler angles.
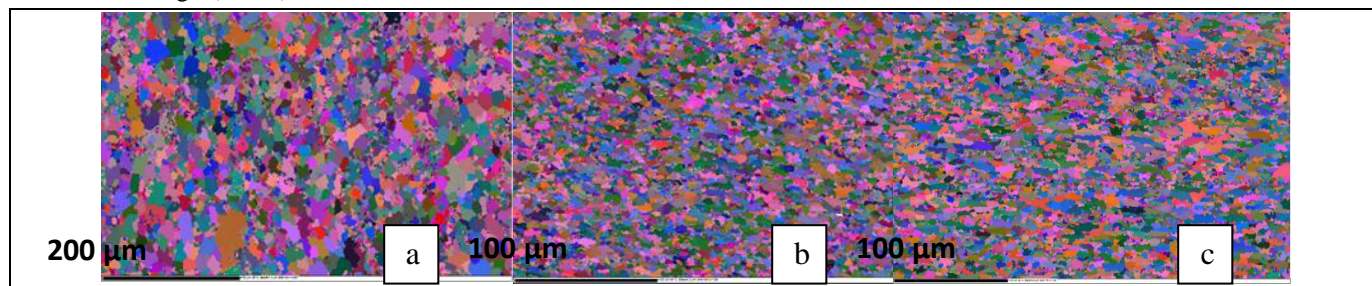
Software: Tango (EBSD)

Fig.8: Preferential crystallographic direction map according to Euler angles for DP780 steel. (a) and (b): outer surface and region along the thickness prior to the bending test; (c): region along the thickness after the sheet metal forming.

According to Euler's map, different colors indicate different crystallographic orientations, so it is verified that for regions a and b of Figure 8, there is no preferential crystallographic orientation before mechanical bending. What exists is a great tangle of dislocations generated by this great variation in the crystallographic orientations and reinforced by the small size of grains, which, because they are smaller, increase the occurrence of dislocations. Therefore, within each of these regions, variation in crystallographic orientation is large. However, when comparing region *a* with region *b*, it is noted that there is not a great difference between the colorations of grains indicating a greater amount of grains oriented in similar crystallographic directions, thus producing similar mechanical responses between the regions *a* and *b*, with fewer obstacles between the outer surface and region along the thickness.

Thus, elastic residual tension finds easier in driving the movement of the dislocations, resulting in a high springback effect, characterized by a decrease in the yield stress during recharging, which constitutes the Bauschinger effect and this type of hardening is known as hardening kinematic. Since mechanical response of crystalline reticulum to the application of tension during loading is different from the response of the reloading step in which the reversal of the direction of deformation occurs, the hardening cannot be isotropic.

Figure 6 reinforces that observed in the Euler maps, since the presence of the three structural fractions in different percentages for each of regions *a* and *b* is verified. It is known that each structural fraction has a preferential crystallographic orientation, so the presence of the three structures at the same time and in considerable percentages results in a high crystallographic variation for region *a* and for region *b*.

These conclusions can be confirmed by the works of some authors [12-14], in which biphasic steels were studied that presented lower levels in the Young's modulus in the direction of the reverse deformation, characterizing the Bauschinger effect. Moreover, in these

works it was observed that all the slip systems in this material were affected by the present dislocations giving rise to a hardening dependent of tangled dislocations or the density of discordances, known as forest hardening.

IV. CONCLUSION

It is possible to affirm that in region of neutral line, the higher value of Von Mises Stress represent the greater amount of elastic residual tension in this same region, which is responsible for the springback effect and then, it is concluded that the springback effect is directly related to the behavior of deformation in the region of neutral line of the material, since this region by deforming less than the regions of the internal and external surfaces, becomes responsible for the elastic deformation that the material presents after mechanical bending and therefore, responsible for the release of residual internal energies that are the driving force of the springback effect.

It is interesting to note that when an energy is supplied to these materials, it is used to decrease the degree of deformation and to decrease the high level of tension caused by the lamination, as a tendency to return to a condition of greater equilibrium, that is, a condition of lower residual tension between the grains.

Results from the FEA show a high value of Von Mises Stress, in the neutral line region, indicating a greater proximity of the yield stress in the direction of the reverse deformation, thus indicating that the discharge energy was transmitted throughout the elastic zone in the reverse direction, once the yield stress was reached. Then, the energy was transmitted the neutral line to surface. This resulted in the lowest possible value of plastic deformation (PEEQ) on neutral line and consequently in a high plastic deformation (PEEQ) intensity in regions closest to surface and a high degree of springback. And according to literature, this type of energy transmission refers to kinematic hardening.

The DP780 steel showed high intensity of coincident site lattices of high angle, predominant structural fraction of the deformed type, little discrepancy

between the percentages of structural fractions present in the external surface in comparison to the region along the thickness, which resulted in a high level of CSL interface. In addition, it presented small resistance to the flow due to the greater similarity in the crystallographic orientations generated by the tangle of dislocations with small discrepancy between the percentages of structural fractions. Thus, a high level of energy stored in the CSL interface coupled with a lower flow resistance resulted in the high elastic recovery in the neutral line region, which presented the lowest PEEQ value and high springback value, thus indicating a kinematic type hardening due to the forest hardening that leads to the Bauschinger effect.

Therefore, it is concluded that the use of isotropic hardening model, although it was not satisfactory to predict with good accuracy the degree of springback, was useful to identify the elasto-plastic behavior of biphasic steel, which was better understood by means of the parameters microstructures obtained with EBSD.

REFERENCES

[1] LAJARIN, S. F. Influência da variação do módulo de elasticidade na previsão computacional do retorno elástico em aços de alta resistência, **acervodigital.ufpr.br**, Ago. 2012, Available in: <http://hdl.handle.net/1884/27466>. Accessed: Mar 2019.

[2] WORLD AUTO STEEL. Advanced High-Strength Steels Application Guidelines Version 6.0. 2017. Available in: <http://www.worldautosteel.org>. Accessed: Jan. 5, 2018.

[3] RAMEZANI, M.; RIPIN, Z. M.; AHMA, R. Modelling of kinetic friction in V-bending of ultra-high-strength steel sheets, **Int J Adv Manuf Technol** (2010) 46:101–110, DOI 10.1007/s00170-008-1450-4.

[4] HASSAN, H. U., TRAPHÖNER, A. G., TEKKAYA, A. Accurate springback prediction in deep drawing using pre-strain based multiple cyclic stress–strain curves in finite element simulation. **International Journal of Mechanical Sciences**, v. 110, p. 229-241, 2016.

[5] HILL, R. A, Theory of yielding and plastic flow of anisotropic metals. **Proc. R. Soc. Lond. Ser. A** 193, 281–297. 1948.

[6] KOMGRIT, L., HAMASAKI, H., HINO, R., YOSHIDA, F. Elimination of springback of high-strength steel sheet by using additional bending with counter punch. **Journal of Materials Processing Technology** 229, p. 199-206. 2016.

[7] YANG, X., CHOI, C., SEVER, N. K., ALTAN, T. Prediction of springback in air-bending of Advanced High Strength Steel (DP780) considering Young's modulus variation and with a piecewise hardening function. **International Journal of Mechanical Sciences** 105, p. 266-272. 2016.

[8] NUMISHEET 2002. Proceedings of the 5th International Conference on Numerical Simulations of 3-D sheet Metal Forming Processes, D-Y. Yang et al. (eds.), Jeju Island, Korea, 2002. Disponível em:<www.numsiheet2002.org>. Acessed: Fev. 8, 2018.

[9] OXFORD INSTRUMENTS HKL. Manual EBSD, 2007. Available in: <www.ebsd.com>. Accessed: Fev.08, 2018.

[10] BRISOLA, Gabriela Martins Souza. Análise da propagação da fratura em modelos coesivos com ométodo dos elementos de contorno. 2018. 1 recurso online (136 p.). **Dissertação (mestrado)** - UniversidadeEstadual de Campinas, Faculdade de Engenharia Civil, Arquitetura e Urbanismo, Campinas, SP.

[11] HU W. An orthotropic yield criterion in a 3-D general stress state, **International Journal of Plasticity**, Volume 21, Issue 9, September 2005, Pages 1771-1796, https://doi.org/10.1016/j.ijplas.2004.11.004.

[12] JINJIN HA, MYOUNG-GYU LEE, FRÉDÉRIC BARLAT, Strain hardening response and modeling of EDDQ and DP780 steel sheet under non-linear strain path, **Mechanics of Materials**, Volume 64, September 2013, Pages 11-26, https://doi.org/10.1016/j.mechmat.2013.04.004.

[13] RUDOLF NEUMANN, SIMONE SCHUSTER, JENS GIBMEIER AND THOMAS BÖHLKE, Two-Scale Simulation of the Hot Stamping Process based on a Hashin-Shtrikman Type Mean Field Model, **Journal of Materials Processing Technology**, 10.1016/j.jmatprotec.2018.11.013, (2018).

[14] ZHONG CHEN, UMESH GANDHI, JINWOO LEE, R.H. WAGONER, Variation and consistency of Young's modulus in steel, **Journal of Materials Processing Technology**, Volume 227, January 2016, Pages 227-243, https://doi.org/10.1016/j.jmatprotec.2015.08.024.